SF2A 2015
F. Martins, S. Boissier, V. Buat, L. Cambrésy and P. Petit (eds)

NUMERICAL SIMULATIONS OF AXISYMMETRIC BONDI-HOYLE ACCRETION ONTO A COMPACT OBJECT

I. El Mellah[1] and F. Casse[1]

Abstract. Compact bodies which are not at rest compare to an homogeneous ambient environment are believed to undergo Bondi-Hoyle axisymmetric accretion as soon as their relative velocity reaches supersonic levels. Contrary to its spherical counterpart, B-H accretion presents flow structures difficult to analytically derive, hence the need for numerical investigations. The broad dynamics at stake when a tiny compact object engulfs surrounding material at a much larger scale has made numerical consistency a polemical issue as it has prevented both scales to be grasped for reasonable wind velocities. We designed a numerical setup which reconciliates the requirement for finite size accretor with steady states properties of the Bondi-Hoyle flow independent of the size of the inner boundary. The robustness of this setup is evaluated accordingly to predictions concerning the mass accretion rate evolution with the Mach number at infinity and the topology of the sonic surface as determined by Foglizzo & Ruffert (1996). It provides an estimation of the mass accretion rates and thus, of the expected X-ray luminosity for an idealized B-H configuration which might not be too far off for isolated compact objects like runaway neutron stars or hyper-luminous X-ray sources.

Keywords: subject, verb, noun, apostrophe

1 Introduction

Accretion of matter by a gravitationally centred field has been an active topic of study over the last decades, as the X-ray satellites unveiled more and more systems where such an interplay was believed to occur in some way. Starting with the Bondi's spherical model of a non-zero temperature stationary flow at infinity (Bondi 1952) enabled quantitative predictions to be derived but soon turned out to be irrelevant in most astrophysical configurations, where the relative motion of the accreting body compare to the ambient medium did matter : super-giant X-ray binaries (Walter et al. 2015), runaway neutron stars (Cordes et al. 1993), symbiotic binaries (Theuns et al. 1996; de Val-Borro et al. 2009), hyper-luminous X-ray sources Pfahl et al. (2002),... Many interpretations had everything to gain at seeing axisymmetric models of accretion to be developed. Well before X-ray pathfinders, Hoyle, Lyttleton and afterwards, Bondi had laid the foundations of an axisymmetric model of a zero temperature supersonic flow at infinity, henceforward referred to as B-H or wind accretion (Hoyle & Lyttleton 1939; Bondi & Hoyle 1944). It is usually the starting point to investigate the influence of more sophisticated considerations as inhomogeneities (Ruffert 1996, 1999), hydrodynamical terms (Horedt 2000), finite size accretors (Ruffert 1994a), small or large scale magnetic fields (Igumenshchev & Narayan 2002; Igumenshchev 2006; Pang et al. 2011), orbital effects (Theuns & Jorissen 1993), radiative feedback (Park & Ricotti 2013), turbulence (Krumholz et al. 2006), net vorticity (Krumholz et al. 2005), etc ; the wind accreting systems grew as they ramified.

In parallel, the new computational capacities offer us the opportunity to unveil the physical phenomena at stake behind the scenes with the search for numerical setups able to reproduce the observational classification. Numerical simulations of B-H accretion started to blossom in the late 80's with a series of works investigating the influence of the hydrodynamical (HD) terms. The stability of the B-H flow was put into question with numerical results glimpsing various instabilities without being able to agree whether their origin was physical or not (see Foglizzo et al. 2005, and references therein). Progress were made in simulating accretion onto not compact objects but the wide dynamics introduced by the small size of a compact object compare to its gravitational

[1] Laboratoire AstroParticules et Cosmologie - Université Paris 7 Diderot - Paris, France

sphere of influence on non-relativistic winds has prevented numerical simulations to converge to a B-H accretion solution around a compact object up to now. A major theoretical step was undertaken with the study of spherical accretion of a flow with a non vanishing velocity at infinity, mixing ballistic and pressure effects all together (Theuns & David 1992). The same blending remained to be done for axisymmetric geometries until Foglizzo & Ruffert (1996), henceforth FR96, linked the sonic surface* of a B-H flow to the simpler one of the spherical configuration.

In this proceeding, our primary goal is to describe a robust axisymmetric numerical setup we designed to take the most of the high performance computing methods implemented in the MPI-parallelized Adaptive Mesh Refinement Versatile Advection Code (MPI-AMRVAC). We constantly monitored our results to compare them to firmly established analytical constraints, derive accurate numerical mass accretion rates and study the steady state structure of the flow (transverse profiles, sonic surface...). Using a continuously nested logarithmic mesh with a shock-capturing algorithm and specific boundary conditions, we can resolve the flow from the vicinity of the central compact object up to the significant deflection scale, at an affordable computational price and with realistic wind velocities. According to the properties of B-H accretion on finite size objects recalled in Ruffert (1994a), we can finally reach numerical regimes where the size of the inner boundary no longer alters the flow properties. We solve the full set of HD Eulerian equations, including the energy one, with the less restrictive adiabatic assumption instead of considering a polytropic flow and identifying the adiabatic and the polytropic indexes. We investigate the evolution of the properties of the B-H accretion flows we obtain with the Mach number of the flow at infinity, from slightly subsonic to highly supersonic setups.

2 Theoretical overview

2.1 The ballistic Hoyle-Lyttleton flow and its Bondi-Hoyle refinement

In their seminal paper, Hoyle & Lyttleton (1939) portrayed a homogeneous supersonic planar flow with a relative velocity and a density at infinity of $\mathbf{v}_\infty$ and ρ_∞, deflected by the gravitational field of a point mass M. As a first approximation, they neglected the influence of the HD terms and solved the equations of motion for a test-mass ; compare to Bondi's spherical model (Bondi 1952), thermodynamics was sacrificed in favour of a more realistic symmetry. In this ballistic framework, the explicit expressions of the trajectories can easily be derived (Bisnovatyi-Kogan et al. 1979). Yet, once the flow reaches the line lying downstream of the gravitational body, dissipative effects are likely to lead to a substantial damping of the orthoradial component of the velocity field, letting the test-mass worn out with a total mechanical energy which turns out to be negative for particles with an impact parameter ζ verifying the Hoyle-Lyttleton accretion condition :

$$\zeta < \zeta_{\rm HL} = \frac{2GM}{v_\infty^2} \tag{2.1}$$

$\zeta_{\rm HL}$ is commonly referred to as the accretion radius or the stagnation point even if, in this picture, particles are left with a non-zero velocity provided by the remaining radial component. G stands for the usual gravitational constant. Given the symmetry of the problem, one can expect that all independent particles in a cylinder of cross section $\pi\zeta_{\rm HL}^2$ will eventually be trapped in the gravitational potential. Those considerations led Hoyle & Lyttleton to suggest an accretion rate of :

$$\dot{M}_{\rm HL} = \pi\zeta_{\rm HL}^2\rho_\infty v_\infty = \frac{4\pi G^2M^2\rho_\infty}{v_\infty^3} \tag{2.2}$$

As a first attempt to include HD effects, accretion column models were developed considering a thin but non zero accretion wake (see Edgar 2004, for a pedagogical review). Those two-flow models (supersonic B-H deflected flow supplying matter and momentum / one-dimensional channelled flow along the column) led to a non linear system of ordinary differential equations describing the dynamics of the accretion column ; investigations of the latter suggested that the position of the stagnation point and thereby, the value of the mass accretion rate, could vary by an order-of-unit factor around the Hoyle Lyttleton mass accretion rate given by (2.2). Yet, for the sake of solvability, those studies either neglected the pressure force in the wake (Edgar 2005) or assumed a polytropic relation between pressure and density to bypass the energy equation (Horedt 2000). In a more pragmatic approach, Bondi was led by the similarities between the spherical and the axisymmetric mass accretion rates

*To be understood as the surface where the flow speed oversteps the local sound speed.

formulae to suggest a first interpolation formula between those asymptotic cases, as a first empirical attempt to account for thermal and kinetic effects all together :

$$\dot{M}_{\rm BH} = \dot{M}_{\rm HL} \left(\frac{{\mathcal{M}_\infty}^2}{{\mathcal{M}_\infty}^2 + 1} \right)^{\frac{3}{2}} \tag{2.3}$$

where $\mathcal{M}_\infty$ is the Mach number of the incoming flow, v_∞ / c_∞.This formula matches the HL mass accretion rate at high Mach numbers but not the Bondi one for low Mach numbers. The non physical origin of this formula led several authors to pinpoint the likely discrepancies which one would observe as soon as a comparison with actual solutions of Eulerian equations are undertaken. The numerical simulations were to confirm this presentiment.

2.2 Sonic surface of Bondi-Hoyle flows

In the spherical Bondi accretion formalism, the sonic radius locates the uniquely determined position where a stationary subsonic inflowing gas becomes supersonic :

$$r_0 = \frac{5-3\gamma}{4} \frac{GM}{c_\infty^2 + \frac{\gamma - 1}{2} v_\infty^2} \tag{2.4}$$

The intrinsic multi-dimensionality of the Hoyle-Lyttleton flow has prohibited until now any comparable level of detail, concerning the analytical properties of the sonic surface, to be reached. FR96 started to bridge the analytical gap between the spherical Bondi accretion of a flow at rest at infinity and the ballistic pressureless Hoyle-Lyttleton accretion, as they proved a topological property of the sonic surface of B-H flows in relation with the radius of their isotropic counterpart, r_0, with the same Bernoulli's invariant value. They showed that the B-H sonic surface must intersect at least once the sphere of radius r_0. The main analytical constrain entailed by this property is the necessity for the sonic surface of flows with $\gamma = 5/3$ to be anchored into the inner boundary of a simulation, whatever its size since the sonic radius vanishes. FR96 also derived an interpolation formula based on asymptotic expansions near the accretor and considerations about the sonic surface. They suggest, providing an unknown constant of unity-order, that the interpolation formula they determined could fit the stationary mass accretion rates measured.

2.3 Designing a Bondi-Hoyle axisymmetric setup

We derive the structure of the B-H flow relying on the MPI-AMRVAC code, further described in Porth et al. (2014). Briefly, the MPI-AMRVAC package consists in a multi-dimensional finite-volume code able to solve, in multiple geometries, the set of equations of hydrodynamics or magnetohydrodynamics for an ideal gas, either in a classical or relativistic framework. In the present proceeding, we called upon a shock-capturing second order in time and space Total Vanishing Diminishing Lax-Friedrichs (TVDLF) scheme and a Koren slope limiter (Koren 1993) to solve the conservative HD equations. So as to properly physically handle the shock, we relax the polytropic assumption and consider the adiabatic energy equation, which might already unveil results beyond the theoretical expectations. Indeed, the main drawback of the polytropic assumption is to add an additional degree of freedom with the polytropic index Γ. Γ has no reason to be equal to the adiabatic index γ (determined by the chemical nature of the flow), as long as the flow is not isentropic (Horedt 2000), which is not our case here because of the expected shock formation. If this founding hypothesis alleviates the introduction of an additional degree of freedom, the price to pay is to refrain the comparison of our results to prediction relying on $\gamma = 5/3$ for it is the adiabatic index of any flow hot enough to be composed of monoatomic (if not, ionized) particles. It also encloses our reflection to compact objects undergoing *adiabatic* wind accretion.

Since the current proceeding reports on axisymmetric properties of the B-H flow, we can work on a spherical 2.5D mesh, where the third component is the longitudinal one, φ, always null. Thus, the cells do respect the full 3D geometry information but the flow is assumed to be invariant by rotation around the polar axis, which spares the mesh to span a third dimension. The incoming wind velocity at infinity is then collinear to the polar axis. Given the reported reasonable stability of the 3D B-H flow against transverse instabilities as the "flip-flop" one at stake in some 2D cylindrical B-H configuration (Blondin & Pope 2009), both theoretically (Soker 1990) and numerically (Blondin & Raymer 2012), we expect such a configuration to give birth to a relatively robust equilibrium from which full 3D simulation should not depart much.

A regular 2.5D spherical grid would suffer two major drawbacks. First, to get a decent radial resolution next to the inner boundary, we would have to work with a huge number of radial cells, which would be painfully time-consuming and would not tell us much more about the relevant dynamics. In addition, the cell aspect ratio $\Delta r/r\Delta\theta$ cannot remain constant all along a radius ; r varying from the inner to the outer boundary by a factor 10^2 to 10^4 (depending on the simulation), a regular grid would give highly deformed cells. As indicated by its name, MPI-AMRVAC presents the capacity to adaptively refine the mesh where needed. A safer swindle (initially introduced for B-H flows by Fryxell & Taam 1988) is to work with a constant aspect ratio, in other words, with a radial step proportional to the radius (hence the " logarithmic grid" designation). It enables us to keep a homogeneous "relative resolution", from the vicinity of the compact object up to the accretion radius. We typically work with $N_\theta = 64$ latitudinal cells and $N_r = 128$,176 or 224 radial cells, depending on the size of the inner radius of the grid ; once the latter is set, we tune the aspect ratio around the unity value to make the outer radius approximately constant from a simulation to another. Given the angular resolution, this approach leads to a radial cell size of the order of a twentieth of the inner boundary one next to it.

The Eulerian equations are associated with usual polar symmetry and antisymmetry conditions along the polar axis. For the outer radial boundary conditions, far ahead the shock, where the flow is supersonic, we prescribe the ballistic solution for v_r and v_θ and the permanent regime solution deduced for ρ from the mass conservation equation by Bisnovatyi-Kogan et al. (1979). We extended the latter to the total specific energy density e. It assures that the gravitational ballistic deflection of the initially planar flow, from infinity to the outer boundary, is taken into account. The downstream outer boundary condition is a continuous one and to avoid any spurious reflection of pressure waves, we set its size $r_{\rm out}$ such as the velocities at the boundary are supersonic. Typically, it requires $r_{\rm out} \sim 8\zeta_{\rm HL}$.

Concerning the inner boundary conditions, much caution must be taken. Straightforward absorbing conditions (floor density and continuous velocities e.g., provided they leave the simulation space) do alter the stability of the flow without guarantee of fitting the continuity of the radial flows. One has to not prevent the stationary solution the mass and energy continuity equations to be achieved, e.g. by ensuring the continuity of $\rho v_r r^2$ at the inner boundary : so as to do so, we computed the density in the inner ghost cells with a first order Taylor-Young expansion and deduced the corresponding radial velocities from the continuity of the radial mass flux $\rho v_r r^2$. For the total specific energy e, the conserved quantity is given by the Bernoulli's condition considered for a permanent flow : $(e + P + \rho\varphi)v_r r^2$. The value of v_θ is much less critical and is also set via a simple first order expansion. Such inner boundary condition entitle the flow to reach a permanent regime as the ones described further.

3 Results and comments

3.1 Structure of the shock and sonic surface

First comments can be made about the large scale geometry of the shocks we obtained. Whatever the Mach number as long as we deal with a supersonic unperturbed flow at infinity, the shock is clearly detached, with a shock front at a distance of the compact object large compare to the size of the inner boundary but of the order of a fraction of the critical impact parameter $\zeta_{\rm HL}$. The opening angle of the shock evolves along the axis, with a concave shape for the shock and smaller opening angles for larger Mach numbers. Concerning the transverse profiles in the tail, we first notice that the shock forms a hollow cavity, in agreement with one of the solutions proposed by Bisnovatyi-Kogan et al. (1979).

Although immune against non axisymmetric instabilities as the flip-flop one, our simulations could lead to longitudinal or axisymmetric transverse instabilities (Cowie 1977; Foglizzo et al. 2005). However, the relative distance to the previous state - defined as the standard deviation point by point between the state values (mass density, impulsion, total specific energy density) at a given time step and the previous one - tends to be smaller than 0.0001% once the steady state is reached : no acoustic cycle takes place to maintain or amplify an oscillation in the tail, in spite of the actual production of entropy at the detached shock interface. This stability of the bow shock should not be attributed to an accretor too large given the ratios $\zeta_{\rm HL}/r_{\rm in}$ we used but might be linked to a solver excessively diffusive or a spatial resolution too low.

We observe a slight beaming effect along the pole in the B-H simulated flow, probably due to a mesh-alignment effect. We believe it essentially alters neither the conclusions we came to nor the trends we derive for the mass accretion rate or the geometry of the shock for instance. Yet, it must be acknowledged that the quantitative information concerning the latter one might give slightly underestimated positions of the forward shock because of a numerical driving in of artificially focused flow along the axis.

The main result concerning the small scale structure of the flow concerns the aforementioned sonic surface. Our simulations confirm Foglizzo and Ruffert's analytical prediction about the topology of the sonic surface for an adiabatic flow with $\gamma = 5/3$: whatever the size of the inner boundary (left panel of Figure 2 and right panel of Figure 1) or the Mach number of the flow, the sonic surface is always anchored into the inner boundary. It extends along the wake of the accretor, the axisymmetry of the cause being preserved in the consequence. For supersonic flows, the density distribution is mostly isotropic and the streamlines, radial, in the vicinity of the inner boundary. Thus, the accretion is regular in the sense that there is no infinite mass accretion rate direction, although the local mass accretion rate is enhanced by a factor of a few in the back hemisphere compare to the front hemisphere. As a consequence, the non isotropy of the mass accretion rates around the inner boundary is mostly due to the non isotropy of the velocity field ; along the mock accretion line, in the wake of the accretor, the flow has been more reaccelerated than upstream after the shock.

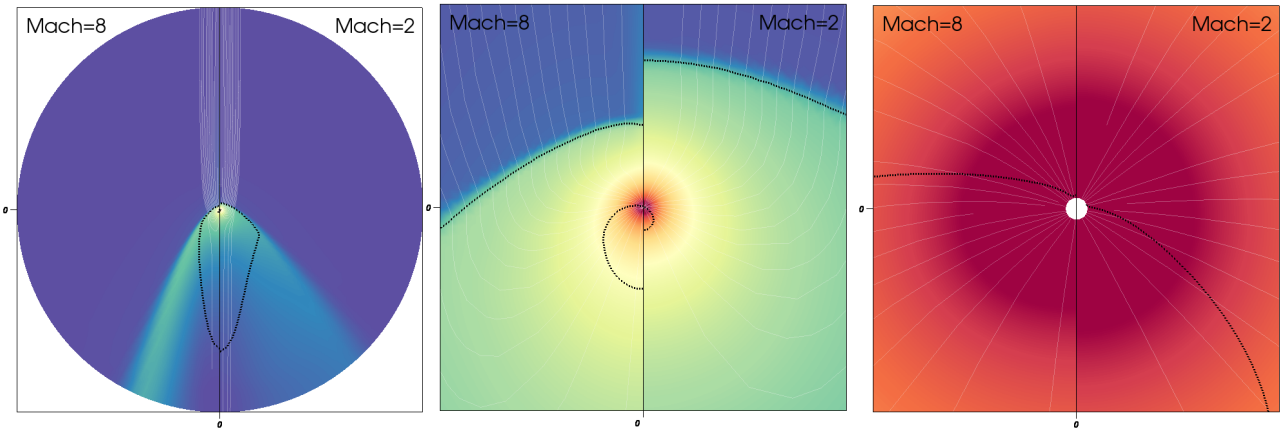

Fig. 1. Logarithmic colour maps of the density for $\mathcal{M}_\infty = 8$ (left panels) and $\mathcal{M}_\infty = 2$ (right panels). Streamlines have been represented in solid white within the accretion cylinder and the dotted black contours stand for Mach-1. Zoom in on the central area by a factor of 20 (centre) and 400 (right).

3.2 Global mass accretion rates

To compare the steady state mass accretion rates at any Mach number, we introduced a homogeneous normalisation variable $\dot{M}_0$ to prevent any privileged point of view between the low and the high $\mathcal{M}_\infty$. The steady-state mass accretion rates $\langle \dot{M} \rangle$ are computed by averaging the instantaneous ones (i.e. the spatially averaged mass accretion rates in the vicinity of the inner boundary, well below the shock front radius) for $t > 10$ crossing-times, once the steady state is reached. The obtained $\langle \dot{M} \rangle$ are presented in the right panel of Figure 2. Data dispersion is dominated by systematics whom influence is given by the two sets of points from the different inner boundary sizes. As expected, the traditional Bondi formula, in blue dotted, matches the Hoyle-Lyttleton mass accretion rate at high Mach numbers, which itself turns out to be an overestimation of the actual mass accretion rate by approximately 30% : it is consistent with the previous reports of $\dot{M}_{\rm HL}$ being a slight overestimation of the numerically observed mass accretion rates in the asymptotically supersonic regime - see, e.g., Figure 7 of Edgar (2004). Yet, since (2.3) does not properly include thermodynamics (e.g. it does not depend on the adiabatic index), it is a poor estimation in the subsonic regimes, overestimating $\dot{M}$ by a factor up to 4 for $\gamma = 5/3$.

Foglizzo and Ruffert's interpolation formula, represented in red dashes in the right panel of Figure 2, is given by the following interpolation formula :

$$\dot{M}_{\rm FR} = \dot{M}_{\rm B} \left[\frac{(\gamma+1)\,{\mathcal{M}_{\rm eff}}^2}{2+(\gamma-1)\,{\mathcal{M}_{\rm eff}}^2} \right]^{\frac{\gamma}{\gamma-1}} \left[\frac{\gamma+1}{2\gamma{\mathcal{M}_{\rm eff}}^2-\gamma+1} \right]^{\frac{1}{\gamma-1}} \tag{3.1}$$

with $\mathcal{M}_{\rm eff}$ the effective Mach number which depends on a free parameter λ assessing the aforementioned discrepancy between $\dot{M}_{\rm HL}$ and the observed mass accretion rate at high $\mathcal{M}_\infty$:

$$\dot{M}_{\rm FR} \xrightarrow[\mathcal{M}_\infty \to \infty]{} \lambda \dot{M}_{\rm HL} \tag{3.2}$$

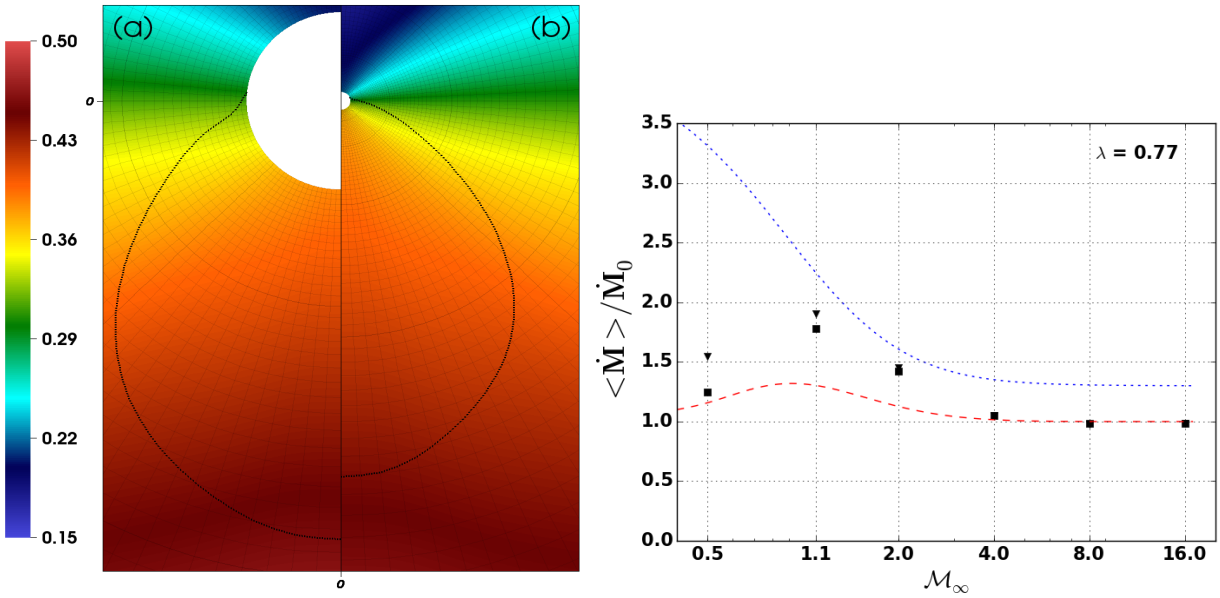

Fig. 2. Left : Colour map of the mass accretion rate for $\mathcal{M}_\infty = 2$ and, for (a), $r_{\rm in} = 10^{-2}\zeta_{\rm HL}$ and for (b), $r_{\rm in} = 10^{-3}\zeta_{\rm HL}$. The scale is linear (arbitrary units) and the inflowing mass is counted positively. The thick dotted black line is the sonic surface, anchored into the inner boundary in both cases. The radial logarithmic mesh is over plotted. Zoom in by a factor 500 on the central area of the simulation. **Right :** Mass accretion rates $\dot{M}$ as a function of the Mach number $\mathcal{M}_\infty$, normalized with the empirical mass accretion rate $\dot{M}_0$. In black are the numerically computed ones for $\zeta_{\rm HL}/r_{\rm in} = 10^2$ (triangles) and $\zeta_{\rm HL}/r_{\rm in} = 10^3$ (squares). The blue dotted line is the Bondi interpolation formula and the red dashed is the FR96's one.

$$\frac{\mathcal{M}_{\rm eff}}{\mathcal{M}_\infty} \sim \frac{1}{2\gamma\lambda^{\frac{\gamma-1}{2}}}\sqrt{\frac{2}{\gamma}}\frac{(\gamma+1)^{\frac{\gamma+1}{2}}}{(\gamma-1)^{\frac{5(\gamma-1)}{4}}\,(5-3\gamma)^{\frac{5-3\gamma}{4}}} \tag{3.3}$$

Physically, λ accounts for an essential non-ballistic feature of the flow, whatever high the Mach number can be. Foglizzo and Ruffert's formula must be understood as a lower limit since it neglects the matter being accreted from a subsonic region whom angular extension becomes larger as $\mathcal{M}_\infty$ decreases.

Although pretty similar to Ruffert's numerical conclusions (Ruffert 1994b; Ruffert & Arnett 1994), our results do not show any decreasing trend at high Mach number and match the interpolation formula $\dot{M}_{\rm FR}$ in the asymptotically supersonic regime for $\lambda \sim 0.77$, down to $\mathcal{M}_\infty = 4$, at a few percents precision level. We also grasp the main feature of the axisymmetric B-H accretion flow that is to say an amplification by a few 10% of $\dot{M}$ around $\mathcal{M}_\infty = 1$ compare to the interpolation formulae (3.1) and the expression of $\dot{M}_0$ verifying $\dot{M} \xrightarrow{\mathcal{M}_\infty \to 0} \dot{M}_{\rm B}$ and $\dot{M} \xrightarrow{\mathcal{M}_\infty \to \infty} \sim \dot{M}_{\rm HL}$. It must be noticed that for $\mathcal{M}_\infty = 0.5$, 1.1 & 2, the mass accretion rates measured are not yet independent of the inner boundary size, which is in agreement with the zero value of the sonic radius : since the sonic surface is anchored into the accretor, there is always directions of accretion where the flow is not supersonic. The smaller the inner boundary size, the closer the simulation from the model drawn in FR96, which is confirmed by the data being closer from their interpolation formula for $r_{\rm in} = 10^{-3}\zeta_{\rm HL}$ than for $r_{\rm in} = 10^{-2}\zeta_{\rm HL}$. It can also be seen from direct visualization of the sonic surface which tends to occupy an angular region around the inner boundary larger for smaller inner boundary radii. Given those elements, those numerical $\dot{M}$ must be seen as upper limits of the ones one would get for a smaller absorbing inner boundary.

4 Conclusions

Numerical simulations with an inner boundary size smaller than 10^{-3} critical impact parameter $\zeta_{\rm HL}$ converge towards common steady states. Given the mass accretion rates we could compute from the latter, we can affirm that the mass interpolation formula derived in FR96 turns out to grasp the qualitative behaviour of flows with a

Mach number at infinity around 1, even if the neglecting of the mass accreted from the subsonic directions makes it an underestimation by a few 10%. The numerical robustness of our results is confirmed by the accordance between the large and small scale properties of the flow, in particular the geometry of the sonic surface : in agreement with FR96's topological comment on the latter, we find sonic surfaces systematically anchored into the inner boundary as soon as the flow is supersonic at infinity.

The present study has discarded the orbital effects like the ones present in binaries (see Theuns & Jorissen 1993; Theuns et al. 1996, for SPH simulations). Yet, if the orbitally induced torque remains small enough, those axisymmetric simulations are not expected to depart much from the actual configuration of Super-giant X-ray binaries where the mass transfer is believed to occur mainly through fast stellar winds. Thanks to our numerical setup, which reconciles the requirement for physical size of the accretor together with the necessity to include the accretion radius within the simulation space, we can start to consider the wind accretion of angular momentum in full 3D simulations in order to unveil the properties of the possibly subsequently formed accretion disc.

We gratefully thank Thierry Foglizzo for fruitful exchanges and the MPI-AMRVAC development team, in particular Oliver Porth, Rony Keppens and Zakaria Meliani, for useful assistance. IEM thanks the organizing committee of the *Journées de la SF2A 2015* for giving him the occasion to present his results at the Paul Sabatier University of Toulouse. We acknowledge the financial support from the UnivEarthS Labex program of Sorbonne Paris Cite (ANR-10-LABX-0023 and ANR-11-IDEX-0005-02).

References

Bisnovatyi-Kogan, G. S., Kazhdan, Y. M., Klypin, A. A., Lutskii, A. E., & Shakura, N. I. 1979, Sov. Astron., 23
Blondin, J. M. & Pope, T. C. 2009, Astrophys. J., 700, 95
Blondin, J. M. & Raymer, E. 2012, Astrophys. J., 752, 30
Bondi, H. & Hoyle, F. 1944, Mon. Not. R. Astron. Soc., 104, 273
Bondi, . 1952, Mon. Not. R. Astron. Soc., 112
Cordes, J. M., Romani, R. W., & Lundgren, S. C. 1993, Nature, 362, 133
Cowie, . 1977, Mon. Not. R. Astron. Soc., 180, 491
de Val-Borro, M., Karovska, M., & Sasselov, D. 2009, arXiv.org, 1148
Edgar, R. G. 2004, New Astron. Rev., 48, 843
Edgar, R. G. 2005, Astron. Astrophys., 434, 41
Foglizzo, T., Galletti, P., & Ruffert, M. 2005, Astron. Astrophys., 2201, 15
Foglizzo, T. & Ruffert, M. 1996, Astron. Astrophys., 361, 22
Fryxell, B. a. & Taam, R. E. 1988, Astrophys. J., 335, 862
Horedt, G. P. 2000, Astrophys. J., 541, 821
Hoyle, F. & Lyttleton, R. A. 1939, Math. Proc. Cambridge Philos. Soc., 35, 405
Igumenshchev, I. V. 2006, Astrophys. J., 649, 31
Igumenshchev, I. V. & Narayan, R. 2002, Astrophys. J., 566, 137
Koren, B. 1993, Notes Numer. Fluid Mech., 45, 117
Krumholz, M. R., McKee, C. F., & Klein, R. I. 2005, Astrophys. J., 618, 757
Krumholz, M. R., McKee, C. F., & Klein, R. I. 2006, Astrophys. J., 638, 369
Pang, B., Pen, U.-L., Matzner, C. D., Green, S. R., & Liebendörfer, M. 2011, Mon. Not. R. Astron. Soc., 415, 1228
Park, K. & Ricotti, M. 2013, Astrophys. J., 767, 163
Pfahl, E., Rappaport, S., & Podsiadlowski, P. 2002, Astrophys. J., 571, L37
Porth, O., Xia, C., Hendrix, T., Moschou, S. P., & Keppens, R. 2014, Astrophys. J. Suppl. Ser., 214, 4
Ruffert, M. 1994a, Astrophys. J., 427, 342
Ruffert, M. 1994b, Astron. Astrophys. Suppl. 106
Ruffert, M. 1996, 814, 793
Ruffert, M. 1999, 06, 17
Ruffert, M. & Arnett, D. 1994, Astrophys. J., 427, 351
Soker, N. 1990, Astrophys. J., 358, 545
Theuns, T., Boffin, H., & Jorissen, A. 1996, 000, 13
Theuns, T. & David, M. 1992, Astrophys. J., 384, 587
Theuns, T. & Jorissen, A. 1993, Mon. Not. R. Astron. Soc., 265, 946
Walter, R., Lutovinov, A. A., Bozzo, E., et al. 2015, eprint arXiv:1505.03651 [arXiv] arXiv:1505.03651v1